

Accelerating exponential integrators to efficiently solve advection-diffusion-reaction equations

Marco Caliari* Fabio Cassini† Lukas Einkemmer‡ Alexander Ostermann§

March 29, 2023

Abstract

In this paper we consider an approach to improve the performance of exponential integrators/Lawson schemes in cases where the solution of a related, but usually much simpler, problem can be computed efficiently. While for implicit methods such an approach is common (e.g. by using preconditioners), for exponential integrators this has proven more challenging. Here we propose to extract a constant coefficient differential operator from advection-diffusion-reaction equations for which we are then able to compute the required matrix functions efficiently. Both a linear stability analysis and numerical experiments show that the resulting schemes can be unconditionally stable. In fact, we find that exponential integrators and Lawson schemes can have better stability properties than similarly constructed implicit-explicit schemes. We also propose new Lawson type integrators that further improve on these stability properties. The effectiveness of the approach is highlighted by a number of numerical examples in two and three space dimensions.

Keywords: Exponential integrators, stiff problems, evolutionary PDEs, advection-diffusion-reaction equations, fast Fourier transform based solvers, μ -mode integrator.

MSC codes: 65L05, 65M06, 65M20, 65M70

1 Introduction

Solving time dependent Partial Differential Equations (PDEs) efficiently is important for better understanding many phenomena in science and engineering. In most cases, in particular for problems which are diffusion dominated, discretizing such PDEs in space results in a very stiff set of Ordinary Differential Equations (ODEs) for which explicit integrators have to take extremely small time steps.

The standard approach to reduce the computational effort for such problems is to use implicit methods. This kind of methods, from a theoretical point of view, can have very attractive properties. In particular, many implicit methods are *unconditionally stable*. Since we are mostly interested in diffusion dominated problems in this paper, we consider methods that are

*Department of Computer Science, University of Verona, Verona, Italy.
E-mail address: marco.caliari@univr.it

†Department of Computer Science, University of Verona, Verona, Italy.
E-mail address: fabio.cassini@univr.it

‡Department of Mathematics, University of Innsbruck, Innsbruck, Austria.
E-mail address: lukas.einkemmer@uibk.ac.at

§Department of Mathematics, University of Innsbruck, Innsbruck, Austria.
E-mail address: alexander.ostermann@uibk.ac.at

unconditionally stable in the sense that they do not have a time step restriction when applied to the linear problem

$$u'(t) = Au(t),$$

where A is a matrix with negative eigenvalues. That is, the time step size is only dictated by the prescribed tolerance (i.e., accuracy), but not by stability considerations. However, implicit methods in general require the solution of a nonlinear set of equations at each time step. This is usually done either by performing Newton iteration in combination with some linear solver or by directly using an IMplicit-EXplicit (IMEX) scheme, which treats implicitly only the linear part of the system. Thus, using implicit methods shifts all the difficulty into finding an efficient way to solve dense linear systems of moderate size (such as those coming from pseudospectral techniques) or large and sparse ones (such as those stemming from finite differences or finite elements spatial discretizations). When the arising linear system is solved by a direct method such as LU decomposition the computational complexity of the obtained algorithm is usually worse than that of an explicit integrator. Otherwise, Krylov subspace based iterative methods are used, such as the Conjugate Gradient (CG) method or the Generalized Minimal RESidual method (GMRES) [27]. For diffusion dominated problems Krylov methods already significantly reduce the computational effort needed. However, for a number of problems preconditioners can be constructed that further reduce the computational effort. Preconditioners transform the linear system in such a way that the solution of the resulting linear system requires fewer iterations. While there are preconditioners that, at least in principle, can be applied generically (e.g. ILU or the celebrated algebraic multi-grid approach [30]), for many challenging problems purpose-built preconditioners have to be constructed. Often such preconditioners use the solution of a related, but simpler, problem that can be solved efficiently (see, e.g., physics based preconditioners [10, 26] or block preconditioners [2, 13]).

Exponentials integrators (see reference [20] for a review) are another way to solve in time stiff differential equations. In this case a linear part of the problem is treated *exactly*, while the nonlinear remainder is treated in an explicit manner. For example, to solve the equation

$$\partial_t u(t) = Au(t) + g(t, u(t))$$

it is possible to use the exponential Euler method

$$u^{n+1} = u^n + \tau \varphi_1(\tau A)(Au^n + g(t^n, u^n)),$$

where A is a linear operator/matrix, τ is the time step size, and $\varphi_1(z) = (e^z - 1)/z$ is an entire function (the singularity at 0 is removable). Even for nonlinear problems, exponential integrators require no Newton iteration, but rather the computation of the action of matrix functions related to the exponential (such as the φ_1 function above) at each time step. If only matrix exponentials are used we call such methods Lawson schemes [21]. The main difficulty for exponential integrators is the evaluation of the arising exponential-like matrix functions. For that purpose Krylov subspace methods [19], schemes based on Leja interpolation [7, 8], and Taylor methods [1] are commonly used. It has been shown in a number of studies that Krylov or Leja based exponential integrators can be superior to implicit schemes for realistic problems, see, e.g., references [12, 14, 15, 22]. Unfortunately, however, the aforementioned technique of preconditioning to further improve performance does not apply to exponential integrators.

Thus, a natural question that arises is whether the solution of a related, but simpler, problem for which an efficient solution is known can be used in the framework of exponential integrators in order to improve the performance of the scheme. The idea that we pursue in this paper is to choose the linear operator A in such a way that the corresponding matrix functions can be

computed efficiently. In particular, let us consider the variable coefficient advection-diffusion-reaction equation

$$\partial_t u(t, \mathbf{x}) = \nabla \cdot (a(\mathbf{x}) \nabla u(t, \mathbf{x})) + \nabla \cdot (\mathbf{b}(\mathbf{x}) u(t, \mathbf{x})) + r(t, \mathbf{x}, u(t, \mathbf{x})), \quad t \in [0, T], \quad \mathbf{x} \in \Omega \subset \mathbb{R}^d$$

that is equipped with appropriate initial and boundary conditions. If we use

$$Au = \nabla \cdot (a(\mathbf{x}) \nabla u) + \nabla \cdot (\mathbf{b}(\mathbf{x}) u)$$

then we have to resort to general purpose Krylov or Leja based schemes, for instance, to compute the action of $\varphi_1(\tau A)$. However, for constant diffusion tensor and velocity field (i.e. if a and \mathbf{b} are independent of \mathbf{x}) we can use a fast Poisson solver, e.g. Fast Fourier Transform (FFT) based methods. This scales linearly (up to a logarithm) in the number of unknowns. The idea is then to consider the following *equivalent* formulation of the equation

$$\partial_t u(t, \mathbf{x}) = Au(t, \mathbf{x}) + \underbrace{\nabla \cdot (a(\mathbf{x}) \nabla u(t, \mathbf{x})) + \nabla \cdot (\mathbf{b}(\mathbf{x}) u(t, \mathbf{x})) - Au(t, \mathbf{x}) + r(t, \mathbf{x}, u(t, \mathbf{x}))}_{g(t, \mathbf{x}, u(t, \mathbf{x}))},$$

where now A is a constant-coefficient approximation to the original advection-diffusion operator. The hope is that the action of $\varphi_1(\tau A)$ can stabilize the nonlinear term $g(t, \mathbf{x}, u(t, \mathbf{x}))$ of the exponential integrator. The choice of A is clearly not uniquely determined and we will consider how to choose it later in the paper.

Let us note that a similar approach to what we pursue in this paper can also be employed in the context of implicit methods. More precisely, an IMEX scheme can be used. The constant-coefficient approximation operator is treated implicitly (which can be done efficiently using, e.g., Fourier methods), while the nonlinear term is treated explicitly. Such schemes, known in the literature as explicit-implicit-null, were considered for instance in reference [29]. Clearly, the class of operators for which efficient linear solvers are known is not equivalent to the class of operators for which the matrix exponential (and related matrix functions) can be computed efficiently. For example, the recently introduced μ -mode integrator can very quickly compute the action of the exponential of arbitrary d -dimensional Kronecker structured matrices [3, 6], while it is more involved to exploit this structure in a linear solver [11]. On the other hand, if for a specific operator a good preconditioner is known, an efficient linear solver can be constructed, while the same is not necessarily true for computing the corresponding matrix functions.

Let us also mention some related work in the context of computing matrix functions. In reference [9] the fact that the matrix exponential can be written as the solution of a linear differential equation is used to decompose the problem into a “preconditioner” and a correction. An exponential integrator is then used to approximate the resulting system. The preconditioners chosen are all purely algebraic in nature (diagonal, block diagonal, etc.) and are not specifically adapted to the underlying PDE. In reference [28] a rational Krylov subspace is constructed. That is, the inverse of the preconditioner is directly built into the Krylov subspace in order to obtain an approximation space that is well behaved. This approach was later extended to trigonometric operators [18].

In this paper we will first perform a linear stability analysis of the proposed approach. In particular, this will show that exponential integrators can have better stability properties than their corresponding IMEX counterparts. We will also propose a class of methods (called stabilized Lawson schemes) that improve upon the stability properties of the classic Lawson schemes. We investigate the choice of A and show that this can have a drastic influence on performance. We note that in reference [29], in the context of IMEX schemes, the authors employ the smallest amount of diffusion in A that is necessary to guarantee stability. We

do observe a similar behavior for some test examples. However, for different two- and three-dimensional advection-diffusion-reaction equations that we investigate this is not the case. In this context, we propose an efficient approach that can be used to select A in a good way, and we perform a number of numerical investigations with appropriate techniques of evaluating the matrix functions to highlight the efficiency of the proposed exponential methods. Finally, we show that they can outperform their IMEX counterparts in a number of situations.

2 Linear stability analysis

As mentioned in the introduction, we investigate here how to determine the approximation operator A by studying a model equation. In particular, we consider the constant coefficient heat equation

$$\partial_t u = \Delta u \quad (1)$$

on the domain $\Omega = (-\pi, \pi)^d$ with periodic boundary conditions, and we equivalently write

$$\partial_t u = \lambda \Delta u + (1 - \lambda) \Delta u, \quad (2)$$

with $\lambda \in [0, 1]$. Note that in this case the approximation operator is simply

$$A = \lambda \Delta.$$

We note that a similar analysis can be performed for more general operators as long as the eigenvalues lie on the negative real axis. Then, in order to determine the parameter λ we perform a linear stability analysis of the temporal exponential integrator in Fourier space. For the convenience of the reader, all the schemes mentioned and studied in this section are collected in the appendix (formulated for a generic abstract semilinear ODE).

Let us first consider the well-known exponential Euler method, which integrates equation (2) in time as follows

$$u^{n+1} = u^n + \tau \varphi_1(\tau \lambda \Delta) \Delta u^n, \quad (3)$$

where u^n is the numerical solution at time t_n , τ is the time step size and $\varphi_1(z) = (e^z - 1)/z$. Here and throughout the paper we assume without loss of generality that τ is constant. Then we have the following result.

Theorem 2.1. *The exponential Euler scheme (3) is unconditionally stable for $\lambda \geq \lambda^{\text{EE}} = 1/2$.*

Proof. Let us denote $\mathbf{k} = (k_1, \dots, k_d) \in \mathbb{Z}^d$, $k^2 = \sum_{\mu} k_{\mu}^2$, and let $\hat{u}_{\mathbf{k}}^n$ be the \mathbf{k} th Fourier mode of u^n . Then, in Fourier space we have

$$\Phi(z, \lambda) := \frac{\hat{u}_{\mathbf{k}}^{n+1}}{\hat{u}_{\mathbf{k}}^n} = 1 - \varphi_1(-\lambda \tau k^2) \tau k^2 = 1 - \frac{1}{\lambda} + \frac{e^{z\lambda}}{\lambda},$$

where $z = -\tau k^2$. Thus, we have unconditional stability if the stability function $\Phi(z, \lambda)$ satisfies

$$|\Phi(z, \lambda)| \leq 1 \quad \text{for all } z \in (-\infty, 0].$$

Since $\lambda \in [0, 1]$ this implies $\lambda \geq 1/2$, as desired. \square

What Theorem 2.1 tells us is that we still get an unconditionally stable scheme for the heat equation even if we only put half of the Laplacian into A . This is the key observation for the numerical methods that we propose in this paper.

Let us now turn our attention to the Lawson–Euler scheme

$$u^{n+1} = e^{\tau\lambda\Delta}(u^n + \tau(1-\lambda)\Delta u^n), \quad (4)$$

which can alternatively be seen as a Lie splitting where we approximate the second subflow by explicit Euler, that is

$$e^{\tau\lambda\Delta}e^{\tau(1-\lambda)\Delta}u^n \approx e^{\tau\lambda\Delta}(u^n + \tau(1-\lambda)\Delta u^n) = u^{n+1}.$$

For this method we obtain the following result.

Theorem 2.2. *The Lawson–Euler scheme (4) is unconditionally stable for $\lambda \geq \lambda^{\text{LE}} = 0.218$.*

Proof. The stability function satisfies

$$\Phi(z, \lambda) = e^{\lambda z}(1 + (1-\lambda)z).$$

Taking the minimum with respect to z we get

$$z = \frac{1}{\lambda(\lambda-1)}.$$

Plugging this into the stability function we obtain

$$1 - \frac{1}{\lambda} + e^{\frac{1}{1-\lambda}} \geq 0.$$

The result then simply follows by computing the zero of the left-hand side. \square

This shows that there exist methods which are unconditionally stable for values of λ smaller than $\lambda^{\text{EE}} = 1/2$. This is of interest because it is often the case that the accuracy of the method increases as λ decreases (see the experiments in sections 4 and 5). In addition, as mentioned in the introduction, the advantage of using schemes that just employ the exponential function is the following: in certain situations it can be more efficient to compute the exponential than the φ functions (e.g., for exploiting the Kronecker structure or if a semi-Lagrangian scheme is used).

A natural question to ask is if it is possible to construct a numerical method for which the constraint on λ is further reduced. We propose then the following scheme

$$u^{n+1} = u^n + \tau e^{\tau\lambda\Delta}\Delta u^n. \quad (5)$$

We call this first order method the *stabilized Lawson–Euler* scheme, for which we obtain the following result.

Theorem 2.3. *The stabilized Lawson–Euler scheme (5) is unconditionally stable for $\lambda \geq \lambda^{\text{SLE}} = 1/(2e) \approx 0.184$.*

Proof. In this case, the stability function is given by

$$\Phi(z, \lambda) = 1 + ze^{\lambda z}.$$

The stated result then follows immediately. \square

Remark 2.1. A similar analysis can be performed also for other classes of schemes. For example, in reference [29] some IMEX schemes have been analyzed in a fully discretized context. In particular, for the well known backward-forward Euler method

$$(I - \tau\lambda\Delta)u^{n+1} = (I + \tau(1 - \lambda)\Delta)u^n$$

the authors obtain the bound $\lambda \geq \lambda^{\text{BFE}} = 1/2$ for unconditional stability. Moreover, they propose the second order method

$$\begin{aligned} \left(I - \frac{\tau}{2}\lambda\Delta\right)U &= \left(I + \frac{\tau}{2}(1 - \lambda)\Delta\right)u^n, \\ \left(I - \frac{\tau}{2}\lambda\Delta\right)u^{n+1} &= \left(I + \frac{\tau}{2}\lambda\Delta\right)u^n + \tau(1 - \lambda)\Delta U \end{aligned}$$

which has the same stability bound $\lambda \geq \lambda^{\text{IMEX2}} = 1/2$.

Let us now consider some examples of second order exponential integrators. In particular, we start with the following class of exponential Runge–Kutta type schemes for equation (2)

$$\begin{aligned} U &= u^n + c_2\tau\varphi_1(c_2\tau\lambda\Delta)\Delta u^n, \\ u^{n+1} &= u^n + \tau\varphi_1(\tau\lambda\Delta)\Delta u^n + \frac{\tau}{c_2}\varphi_2(\tau\lambda\Delta)(1 - \lambda)\Delta(U - u^n), \end{aligned} \tag{6}$$

where $0 < c_2 \leq 1$ is a free parameter and $\varphi_2(z) = (\varphi_1(z) - 1)/z$. For this scheme we have the following result.

Theorem 2.4. *The exponential Runge–Kutta scheme (6) is unconditionally stable for $\lambda \geq 1/(1 + c_2)$.*

Proof. The stability function is given by

$$\Phi(z, \lambda) = 1 + z\varphi_1(\lambda z) + z^2(1 - \lambda)\varphi_2(\lambda z)\varphi_1(c_2\lambda z).$$

Then, by imposing $|\Phi(z, \lambda)| \leq 1$ for all $z \in (-\infty, 0]$ we have

$$\frac{1 - \lambda}{c_2\lambda} - 1 \leq 0$$

from which we obtain $\lambda \geq 1/(1 + c_2)$ as desired. \square

The smallest result, in terms of unconditional stability, is obtained by setting the free parameter $c_2 = 1$, which yields $\lambda \geq \lambda^{\text{ERK2P2}} = 1/2$.

Let us consider now another class of second order exponential Runge–Kutta integrators, which requires just the φ_1 function. For the model equation (2) this yields

$$\begin{aligned} U &= u^n + c_2\tau\varphi_1(c_2\tau\lambda\Delta)\Delta u^n, \\ u^{n+1} &= u^n + \tau\varphi_1(\tau\lambda\Delta)\Delta u^n + \frac{\tau}{2c_2}\varphi_1(\tau\lambda\Delta)(1 - \lambda)\Delta(U - u^n). \end{aligned} \tag{7}$$

We obtain the following unconditional stability result.

Theorem 2.5. *The exponential Runge–Kutta scheme (7) is unconditionally stable for $\lambda \geq 1/(1 + 2c_2)$.*

Proof. The stability function is given by

$$\Phi(z, \lambda) = 1 + z\varphi_1(\lambda z) + \frac{z^2}{2}(1 - \lambda)\varphi_1(\lambda z)\varphi_1(c_2\lambda z)$$

for which we obtain $\lambda \geq 1/(1 + 2c_2)$ as desired. \square

The choice $c_2 = 1$ yields the bound $\lambda \geq \lambda^{\text{ERK2P1}} = 1/3$, which is smaller than the bound obtained for the previous method.

Concerning the second order Lawson-type schemes, we consider the Lawson2a and the Lawson2b integrators, which integrate equation (2) as follows

$$\begin{aligned} U &= e^{\frac{\tau}{2}\lambda\Delta} \left(u^n + \frac{\tau}{2}(1 - \lambda)\Delta u^n \right), \\ u^{n+1} &= e^{\tau\lambda\Delta} u^n + \tau e^{\frac{\tau}{2}\lambda\Delta} (1 - \lambda)\Delta U, \end{aligned} \quad (8)$$

and

$$\begin{aligned} U &= e^{\tau\lambda\Delta} \left(u^n + \tau(1 - \lambda)\Delta u^n \right), \\ u^{n+1} &= e^{\tau\lambda\Delta} u^n + \frac{\tau}{2} e^{\tau\lambda\Delta} (1 - \lambda)\Delta u^n + \frac{\tau}{2} (1 - \lambda)\Delta U, \end{aligned} \quad (9)$$

respectively. In terms of unconditional stability, we have the following result.

Theorem 2.6. *The Lawson2a scheme (8) and the Lawson2b scheme (9) are unconditionally stable for $\lambda \geq \lambda^{\text{L2A}} = \lambda^{\text{L2B}} = 0.301$.*

Proof. The stability functions are given by

$$\Phi(z, \lambda) = e^{\lambda z} \left(1 + z(1 - \lambda) \left(1 + \frac{z(1 - \lambda)}{2} \right) \right)$$

and

$$\Phi(z, \lambda) = e^{\lambda z} \left(1 + \frac{z}{2}(1 - \lambda) + \frac{z}{2}(1 - \lambda)(1 + z(1 - \lambda)) \right)$$

for Lawson2a and Lawson2b, respectively. In both cases, a numerical calculation leads to the restriction $\lambda \geq 0.301$ for unconditional stability. \square

We now propose a second order variant of the stabilized Lawson–Euler scheme. Letting $0 < \alpha \leq 1$ be a free parameter, we obtain for the model equation (2) the following class of methods

$$\begin{aligned} U &= u^n + \alpha\tau e^{\alpha\tau\lambda\Delta} \Delta u^n, \\ u^{n+1} &= u^n + \tau e^{\frac{\tau}{2}\lambda\Delta} \Delta u^n + \frac{\tau}{2\alpha} e^{\tau\lambda\Delta} (1 - \lambda)\Delta(U - u^n). \end{aligned} \quad (10)$$

We call this second order method the *stabilized Lawson2* scheme, for which we have the following result.

Theorem 2.7. *The stabilized Lawson2 scheme (10) with $\alpha = \alpha^{\text{SL2}} = 0.327$ is unconditionally stable for $\lambda \geq \lambda^{\text{SL2}} = 0.183$.*

Proof. The stability function is given by

$$\Phi(z, \lambda) = 1 + ze^{\frac{\lambda z}{2}} + \frac{z^2}{2}(1 - \lambda)e^{(1+\alpha)\lambda z}.$$

Then, setting $\alpha = \alpha^{\text{SL2}} = 0.327$, a numerical calculation leads to the restriction $\lambda \geq 0.183$ for unconditional stability. \square

Note that the value $\alpha^{\text{SL}2} = 0.327$ is chosen such that the corresponding parameter $\lambda^{\text{SL}2}$ is as small as possible.

In Table 1 we have collected, in descending order, the stability lower bounds of all the methods considered in this section, together with the labels that we will use throughout the paper. To summarize, we find that the stabilized Lawson schemes can be operated with the smallest values of λ , followed by the Lawson schemes. Exponential integrators and IMEX schemes require a larger value of λ to be unconditionally stable.

method	label	order	stab. lower bound
backward–forward Euler	BFE	1	$\lambda^{\text{BFE}} = 1/2$
implicit–explicit2	IMEX2	2	$\lambda^{\text{IMEX2}} = 1/2$
exponential Euler	EE	1	$\lambda^{\text{EE}} = 1/2$
exponential RK2 with φ_2 ($c_2 = 1$)	ERK2P2	2	$\lambda^{\text{ERK2P2}} = 1/2$
exponential RK2 with φ_1 ($c_2 = 1$)	ERK2P1	2	$\lambda^{\text{ERK2P1}} = 1/3$
Lawson2a	L2A	2	$\lambda^{\text{L2A}} = 0.301$
Lawson2b	L2B	2	$\lambda^{\text{L2B}} = 0.301$
Lawson–Euler	LE	1	$\lambda^{\text{LE}} = 0.218$
stabilized Lawson–Euler	SLE	1	$\lambda^{\text{SLE}} = 1/(2e) \approx 0.184$
stabilized Lawson2 ($\alpha^{\text{SL}2} = 0.327$)	SL2	2	$\lambda^{\text{SL}2} = 0.183$

Table 1: Collection of methods, in descending order in terms of unconditional stability. Floating point notation means obtained by numerical approximations.

Remark 2.2. The stabilized Lawson–Euler and the stabilized Lawson2 schemes are *not* exact for linear problems, as opposed to the other exponential integrators. Moreover, it is straightforward to see that they are not A-stable (see Figure 1 for a plot of the A-stability regions). Nevertheless, the stability regions contain the whole negative real axis. Therefore, with both schemes we can treat the Laplacian operator without incurring a time step size restriction.

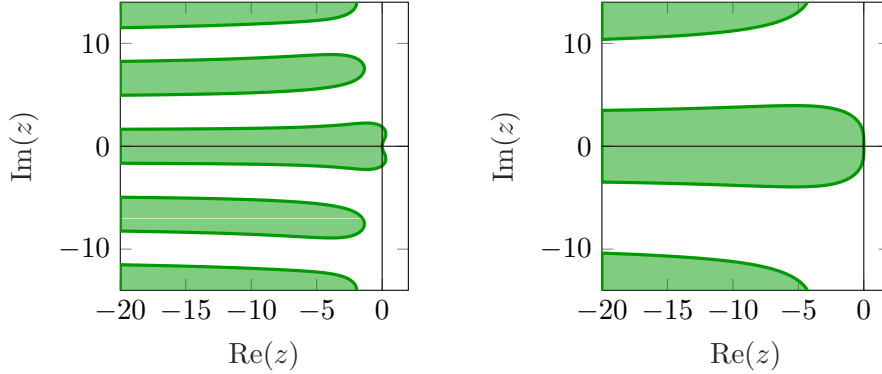


Figure 1: A-stability regions (green) of the SLE method (left) and of the SL2 scheme (right).

3 Accelerated exponential methods

In this section we use the above analysis to propose a choice for the approximation operator A in a more general context. We consider in fact the following advection-diffusion-reaction equation

$$\partial_t u(t, \mathbf{x}) = \nabla \cdot (a(\mathbf{x}) \nabla u(t, \mathbf{x})) + \nabla \cdot (\mathbf{b}(\mathbf{x}) u(t, \mathbf{x})) + r(t, \mathbf{x}, u(t, \mathbf{x})), \quad (11)$$

where $a(\mathbf{x}) \in \mathbb{R}^{d \times d}$ is a diagonal diffusion tensor and $\mathbf{b}(\mathbf{x}) = (b_\mu(\mathbf{x}))_\mu$, for $\mu = 1, \dots, d$, is a velocity vector field, with appropriate boundary and initial conditions on the domain $\Omega \subset \mathbb{R}^d$. We now rewrite equation (11) in the following equivalent form

$$\partial_t u(t, \mathbf{x}) = Au(t, \mathbf{x}) + g(t, \mathbf{x}, u(t, \mathbf{x})), \quad (12a)$$

where

$$Au(t, \mathbf{x}) = \lambda \sum_{\mu=1}^d a_{\mu\mu}^{\max} \partial_{x_\mu x_\mu} u(t, \mathbf{x}) + \boldsymbol{\beta} \cdot \nabla u(t, \mathbf{x}) \quad (12b)$$

and

$$g(t, \mathbf{x}, u(t, \mathbf{x})) = \nabla \cdot ((a(\mathbf{x}) - \lambda a^{\max}) \nabla u(t, \mathbf{x})) + \nabla \cdot ((\mathbf{b}(\mathbf{x}) - \boldsymbol{\beta}) u(t, \mathbf{x})) + r(t, \mathbf{x}, u(t, \mathbf{x})). \quad (12c)$$

Here $\lambda \in [0, 1]$, while a^{\max} and $\boldsymbol{\beta}$ are the diagonal matrix and the vector with components

$$a_{\mu\mu}^{\max} = \max_{\mathbf{x}} a_{\mu\mu}(\mathbf{x}), \quad \beta_\mu = \frac{1}{|\Omega|} \int_{\Omega} (b_\mu(\mathbf{x}) + \partial_{x_\mu} a_{\mu\mu}(\mathbf{x})) d\mathbf{x}, \quad \mu = 1, \dots, d, \quad (12d)$$

respectively. The idea here is that we extract λa^{\max} from the diffusion part of the equation as described in the previous section. In addition, we move into the linear operator also a constant part from the advection term, which is in general beneficial for exponential integrators. We have chosen here to use the average velocity as this physically represents a good constant-coefficient approximation of the advection operator. Moreover, note that we have to take into account not only the advection given by $\mathbf{b}(\mathbf{x})$ but also the advection that is implicitly contained in the diffusion operator.

It is possible now to apply to equation (12a) the methods analysed in section 2 for the linear homogeneous diffusion case and formulated in the appendix for the general case. The required matrix functions/linear solves for A can be efficiently computed in a variety of ways (e.g. using FFT or μ -mode techniques). More details and an investigation of the performance of these schemes will be considered in section 5.

Note that in order to obtain an efficient scheme the choice of the parameter λ is crucial. In reference [29], in the context of IMEX schemes, the authors obtained satisfactory performances choosing λ as small as the stability condition permits. By following this approach, we also observed good results in the numerical validation performed in section 4. However, additional numerical experiments presented in section 5 show that this is not necessarily always the best choice. Thus, we are faced with the task of determining λ in such a way that the error of the numerical approximation is as small as possible. We suggest the following approach. First, we perform a simulation where only a small number of degrees of freedom is used for the space discretization. Using this simulation we perform a parameter scan for the admissible values of λ in order to determine the one that gives the smallest error. Only this λ is then used in the simulation of the advection-diffusion-reaction equation. Note that this procedure has negligible computational cost, since it is performed only for a small problem. Nevertheless, numerical experiments show that the obtained values for λ still give good approximations to the optimal ones which correspond to the highest accuracy of the methods (see, for instance, Figure 4).

4 Numerical validation of the stability constraints

In this section we show that the stability bounds derived for the model equation in section 2 do also apply to more complicated equations. In particular, we will consider a linear and a nonlinear one-dimensional diffusion(-reaction) equation with variable coefficients.

4.1 Linear diffusion

We start by considering the following one-dimensional linear diffusion equation with space dependent coefficients

$$\begin{cases} \partial_t u(t, x) = a(x) \partial_{xx} u(t, x), & x \in (-\pi, \pi), \quad t \in [0, T], \\ u(0, x) = \sin x, \end{cases} \quad (13)$$

subject to periodic boundary conditions. In the experiments we use $a(x) = 1 + 10 \sin^2 x$. As described above, we then rewrite equation (13) as

$$\partial_t u(t, x) = \underbrace{\lambda a^{\max} \partial_{xx} u(t, x)}_{Au(t, x)} + \underbrace{(a(x) - \lambda a^{\max}) \partial_{xx} u(t, x)}_{g(x, u(t, x))}, \quad (14)$$

with $\lambda \in [0, 1]$.

The structure of the equation allows for an effective discretization in space by means of a Fourier spectral technique. In particular, we denote with N the number of Fourier modes. Then, the temporal schemes studied in section 2 and resumed in the appendix can be applied in a straightforward manner, with the computation of derivatives and matrix functions by pointwise operations on Fourier coefficients.

Here, we verify that the theoretical lower bounds for λ found in section 2 also apply to this space dependent coefficients diffusion equation. The actual simulations have been carried out with $N = 2^{12}$ and $T = 1/40$, and the achieved errors for different λ and varying number of time steps $m = 2^\ell$, with $\ell = 4, 6, 8, \dots, 14$, have been measured at the final time T in the infinity norm, relatively with respect to the exact solution of equation (13). The results are collected in Figure 2. First of all, we observe that all the considered exponential methods show the expected order of convergence (in particular also the newly derived stabilized Lawson schemes). Then, we also clearly see that, as λ decreases, some methods fail to be unconditionally stable. In particular, if we compare with the bounds resumed in Table 1, we observe that the values found can be applied sharply also to the case of equation (13). Indeed, up to $\lambda = 0.5$ all the methods are stable. Then, if we further decrease λ , some methods start to blow up when incrementing the number of time steps, in accordance to what presented in Table 1. Then, as predicted by the linear analysis, for $\lambda < \lambda^{\text{SL}2}$ all the methods fail to be unconditionally stable.

4.2 Nonlinear diffusion-reaction

We now turn our attention to the following one-dimensional nonlinear diffusion-reaction equation

$$\begin{cases} \partial_t u(t, x) = \partial_x (a(x) \partial_x u(t, x)) + r(u(t, x)), & x \in (-\pi, \pi), \quad t \in [0, T], \\ u(0, x) = \sin x, \end{cases} \quad (15)$$

in an inhomogeneous medium with periodic boundary conditions, see reference [25]. Here we select $a(x) = 1 + 10 \sin^2 x$ as space dependent diffusion coefficient, and the nonlinearity is of quadratic type $r(u) = u(1 - u)$. Similarly to the previous example, we rewrite equation (15) as

$$\partial_t u(t, x) = \underbrace{\lambda a^{\max} \partial_{xx} u(t, x)}_{Au(t, x)} + \underbrace{\partial_x ((a(x) - \lambda a^{\max}) \partial_x u(t, x)) + r(u(t, x))}_{g(x, u(t, x))}. \quad (16)$$

We first discretize in space with a Fourier spectral method employing $N = 2^{10}$ modes. Then, as for the previous example, the temporal schemes can be applied straightforwardly with pointwise operations on Fourier coefficients. We simulate until the final time $T = 1/10$ with a number of

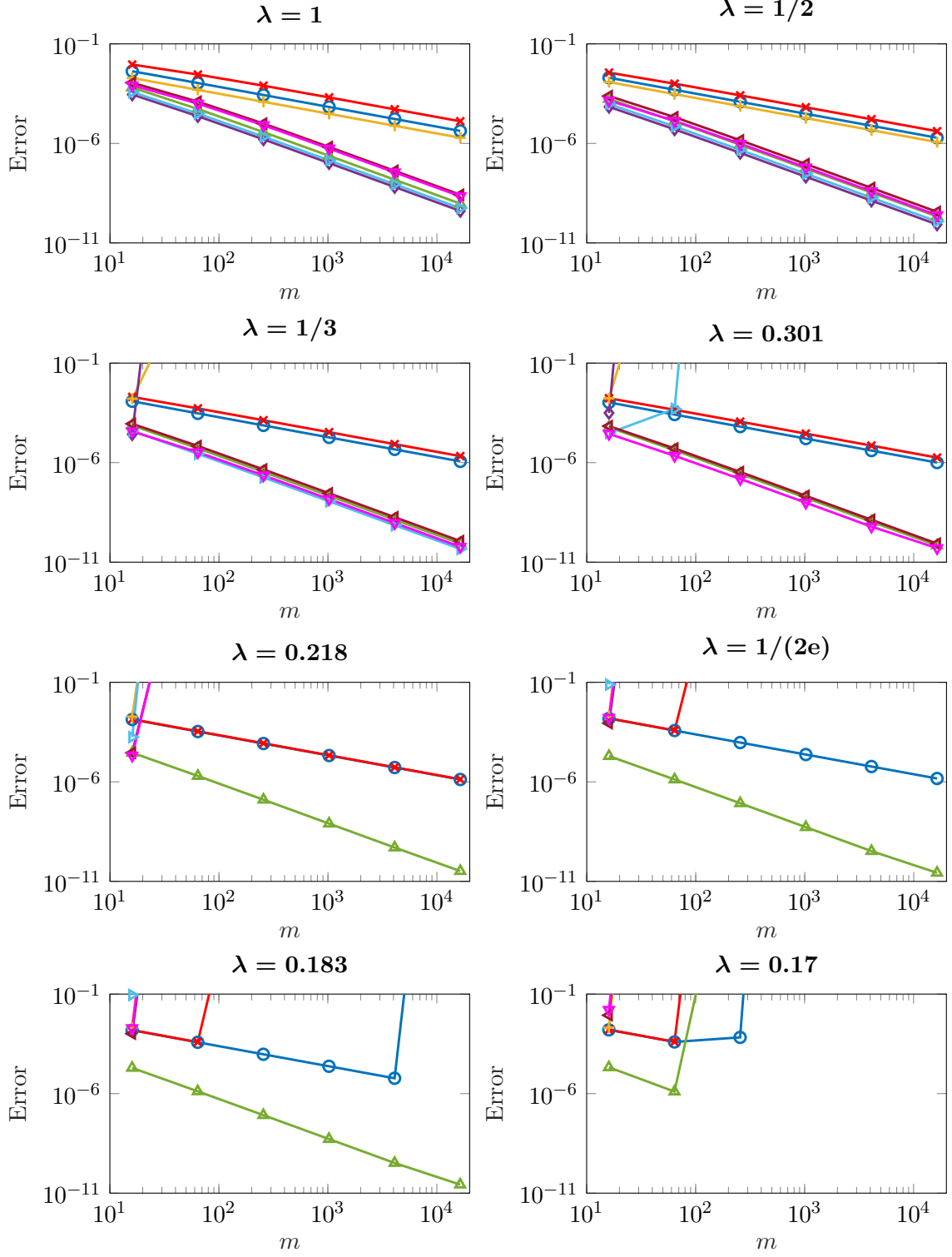


Figure 2: Solution of problem (13) rewritten as equation (14), with different schemes, decreasing λ and varying number of time steps m . The blue \circ line is SLE, the red \times line is LE, the yellow $+$ line is EE, the purple \diamond line is ERK2P2, the green \triangle line is SL2, the light blue \triangleright line is ERK2P1, the brown \triangleleft line is L2A and the magenta ∇ line is L2B.

time steps equal to $m = 2^{12}$ for all the methods. We choose different values of λ and we measure the relative errors in the infinity norm with respect to a reference solution computed with exponential RK2 with φ_2 as time integrator (applied to original equation (15) semidiscretized in space with spectral finite differences, and a sufficiently large number of time steps). We collect the results in Figure 3.

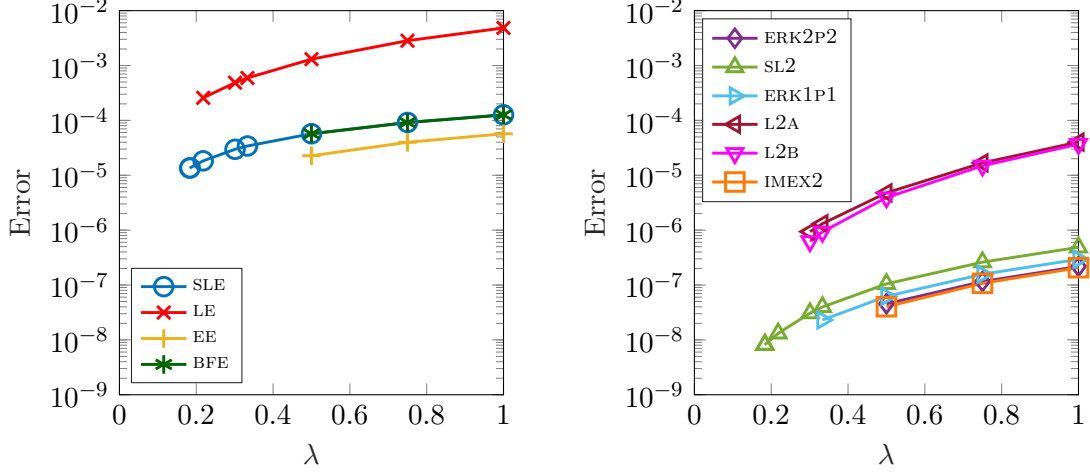


Figure 3: Solution of problem (15) rewritten as equation (16), with different schemes of first order (left), of second order (right) and varying value λ . The number of time steps is fixed to $m = 2^{12}$ for each method. Missing marks mean that the error was above the plot threshold 10^{-2} .

Also in this nonlinear case, we observe that the linear analysis predicts very sharply the amount of diffusion that we can consider in the operator A while keeping unconditional stability. Moreover, it is also clear that each method becomes more precise as the value λ decreases, with in general a greater gain for second order methods than the first order ones. For completeness, we added also the results obtained with the IMEX schemes mentioned in Remark 2.1. Overall, in terms of achieved accuracy, we observe that the stabilized Lawson–Euler and the stabilized Lawson2 schemes perform best among the methods of first and second order, respectively.

5 Performance comparison

In this section, we present performance results on two- and three-dimensional advection-diffusion-reaction equations. All the experiments have been performed on an Intel Core i7-10750H CPU with six physical cores and 16GB of RAM, using Matlab R2022a. Moreover, the errors showed in the plots are always computed in the infinity norm at the final time relatively to a reference solution computed with the Lawson2b integrator and sufficiently small time steps.

For comparison, we perform a “standard” integration of the problem, i.e., we employ the time integrators summarized in the appendix putting the entire diffusion and advection operators in the linear part. The remainder g is then equal to the reaction. In this case we use the general purpose **kiops** method [17], whose Matlab implementation is available at <https://gitlab.com/stephane.gaudreault/kiops/-/tree/master/>. While there are many techniques available to compute the matrix functions [1, 4, 5, 23, 24], **kiops** is generally recognized to be among those who perform best. This routine requires an input tolerance, which we set as $\tau^{p+1}/100$, where τ is the time step size and p is the order of the time integrator. For the IMEX schemes the linear systems are solved with the biconjugate gradient stabilized iterative

method (implemented in the internal Matlab function `bigstab`). Also for this routine we set the input tolerance as $\tau^{p+1}/100$.

5.1 Two-dimensional advection-diffusion-reaction

We start by considering the following two-dimensional advection-diffusion-reaction equation

$$\begin{cases} \partial_t u(t, x_1, x_2) = \nabla \cdot (a(x_1, x_2) \nabla u(t, x_1, x_2)) + \nabla \cdot (\mathbf{b}(x_1, x_2) u(t, x_1, x_2)) + r(u(t, x_1, x_2)), \\ u(0, x_1, x_2) = \exp(-(x_1^2 + x_2^2)) \end{cases} \quad (17)$$

in an inhomogeneous and anisotropic medium with periodic boundary conditions. Here $(x_1, x_2) \in (-3\pi, 3\pi)^2$, $t \in [0, T]$, the diffusion tensor is given by

$$a(x_1, x_2) = \begin{pmatrix} a_{11}(x_1, x_2) & 0 \\ 0 & a_{22}(x_1, x_2) \end{pmatrix} = \begin{pmatrix} \frac{1}{2} + \frac{1}{6} \sin^2(x_1) \sin^2(x_2) & 0 \\ 0 & \frac{1}{2} + \frac{1}{6} \cos^2(x_1) \cos^2(x_2) \end{pmatrix},$$

the velocity field is given by

$$b_1(x_1, x_2) = \frac{1}{5} \sin^2(x_1), \quad b_2(x_1, x_2) = \frac{1}{5} \sin^2(x_2),$$

and the nonlinearity is of quadratic type $r(u) = \frac{1}{4}u(1-u)$. For the proposed approach we then rewrite equation (17) as

$$\partial_t u(t, x_1, x_2) = Au(t, x_1, x_2) + g(x_1, x_2, u(t, x_1, x_2)), \quad (18)$$

see formulas (12). The structure of the equation allows for an effective discretization in space using a Fourier pseudospectral approach. In particular, we consider $N = N_x = N_y$ Fourier modes per direction, and we employ the internal Matlab functions `fft2` and `ifft2` to perform the direct and inverse transforms, respectively, which are based on the highly efficient FFTW algorithm [16]. Note that, once in Fourier space, the application of the relevant matrix functions is simply performed by pointwise operations on the Fourier coefficients.

In order to determine the free parameter λ in the operator A , we follow the approach described in section 3. In fact, we take $N = 2^5$ Fourier modes, $m = 2^8$ time steps and as final simulation time $T = 4$. The results are presented in Figure 4. For comparison, we plot also the results obtained with $N = 2^8$. As we can observe the two plots are very similar, but the upper ones have been obtained with a negligible computational time, still guaranteeing a very good guess for the optimal λ .

A summary of the values of λ obtained in this way for all the integrators under consideration is given in Table 2. Remark that, in this example, it is not always the case that the lower bounds stemming from the linear stability analysis correspond to the lowest errors, both for the exponential and for the IMEX schemes (cf. Table 1).

method	BFE	EE	LE	SLE	ERK2P1	IMEX2	L2A	SL2
value of λ	0.50	0.50	0.22	0.23	0.33	0.57	0.53	0.57

Table 2: Values of λ , for the different schemes that are employed to integrate problem (17) rewritten as equation (18) (see also Figure 4).

Now, employing for each integrator the corresponding value of λ found, we present the actual performance results using $N = 2^8$ degrees of freedom for every spatial variable. As a comparison, we consider the original equation (17) solved numerically with the same temporal

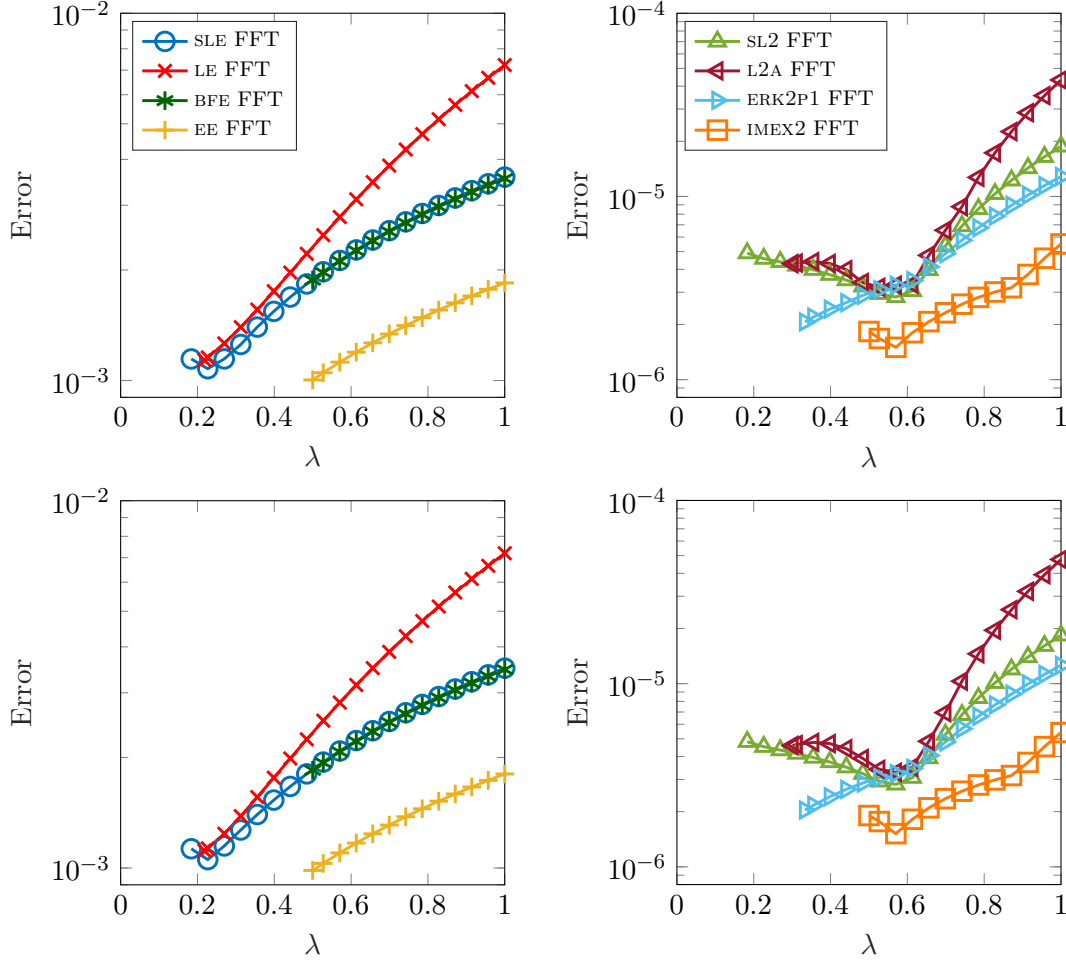


Figure 4: Solution of problem (17) rewritten as equation (18), with different first order schemes (left) and second order schemes (right), for varying value λ . The number of time steps is fixed to $m = 2^8$ for each method, while the number of degrees of freedom for each spatial variable is $N = 2^5$ (top) and $N = 2^8$ (bottom).

integrators and spectral finite differences for the space discretization. The number of time steps is set to 2^{ℓ_1} , with $\ell_1 = 9, \dots, 12$, for the first order integrators, while 2^{ℓ_2} , with $\ell_2 = 8, \dots, 11$, for the second order methods. The final simulation time is again $T = 4$. The results are collected in the CPU diagrams of Figure 5. As we can see, overall the proposed approach allows to obtain slightly better errors with respect to the results in the original formulation. Moreover, the computational time of the proposed approach is less than the corresponding integration in the original formulation. Among the first order schemes the exponential methods perform equally well, while for the second order methods the implicit-explicit2 scheme is the one that shows slightly better results. Note also that, when integrating equation (18) with the proposed approach, the wall-clock time is basically independent of the chosen time integrators, both for first and second order methods. This is expected, as the most costly operations in this case are the Fourier and inverse Fourier transforms, and their number is roughly the same among the first order and the second order schemes, respectively. A summary of the needed transforms per time step for each method is given in Table 3.

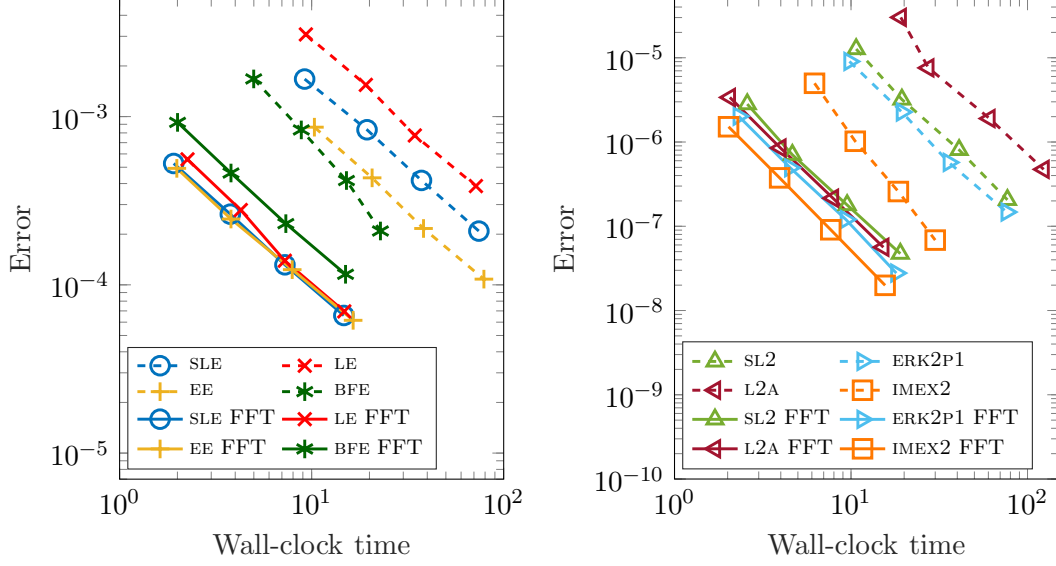


Figure 5: Results for the simulations of problem (17) (dashed lines), rewritten as equation (18) (solid lines), with different integrators of first order (left, number of time steps $m = 2^{\ell_1}$ with $\ell_1 = 9, \dots, 12$) and of second order (right, number of time steps $m = 2^{\ell_2}$ with $\ell_2 = 8, \dots, 11$).

method	BFE	EE	LE	SLE	ERK2P1	IMEX2	L2A	SL2
number of FFTs and IFFTs	7	7	7	7	14	14	15	16

Table 3: Number of Fourier and inverse Fourier transforms needed to perform a time step of equation (18) with selected methods.

5.2 Three-dimensional advection-diffusion-reaction

We now consider the following three-dimensional advection-diffusion-reaction equation

$$\begin{cases} \partial_t u(t, x_1, x_2, x_3) = a(x_1, x_2, x_3) \Delta u(t, x_1, x_2, x_3) + b \sum_{\mu=1}^3 \partial_{x_\mu} u(t, x_1, x_2, x_3) + r(u(t, x_1, x_2, x_3)), \\ u(0, x_1, x_2, x_3) = \left(\frac{27}{4}\right)^3 x_1 x_2 x_3 (1-x_1)^2 (1-x_2)^2 (1-x_3)^2, \end{cases} \quad (19)$$

in the spatial domain $\Omega = (0, 1)^3$ and $t \in [0, T]$. We equip the problem with homogeneous Dirichlet boundary conditions on the set $\{(x_1, x_2, x_3) \in \partial\Omega : x_1 x_2 x_3 = 0\}$ and with homogeneous Neumann boundary conditions elsewhere. We set the diffusion coefficient to

$$a(x_1, x_2, x_3) = \frac{1}{10} e^{-(x_1-1/2)^2 - (x_2-1/2)^2 - (x_3-1/2)^2},$$

while the nonlinearity is of cubic type $r(u) = u(1 + u^2)$.

For the proposed approach we rewrite equation (19) as

$$\begin{aligned} \partial_t u(t, x_1, x_2, x_3) = & \underbrace{(\lambda a^{\max} \Delta + b(\partial_{x_1} + \partial_{x_2} + \partial_{x_3}))u(t, x_1, x_2, x_3)}_{Au(t, x_1, x_2, x_3)} \\ & + \underbrace{(a(x_1, x_2, x_3) - \lambda a^{\max}) \Delta u(t, x_1, x_2, x_3) + r(u(t, x_1, x_2, x_3))}_{g(x_1, x_2, x_3, u(t, x_1, x_2, x_3))}. \end{aligned} \quad (20)$$

We discretize this equation in space with standard second order centered finite differences, using $N = N_{x_1} = N_{x_2} = N_{x_3}$ discretization points for each direction. By doing so, the linear operator A in equation (20) is approximated by a matrix with Kronecker sum structure $A_3 \oplus A_2 \oplus A_1$, where $A_\mu \in \mathbb{R}^{N_{x_\mu} \times N_{x_\mu}}$ is the discretization matrix of the operator $\lambda a^{\max} \partial_{x_\mu x_\mu} + b \partial_{x_\mu}$. Here the symbol \oplus denotes the standard Kronecker sum of matrices. Hence, for those exponential integrators that just require the exponential function (i.e., the ones of Lawson type), it is possible to employ μ -mode based techniques in order to efficiently compute the needed actions of the matrix exponential via Tucker operators, see references [3, 6] for more details.

Similarly to the previous example, in order to determine the free parameter λ in A , we use the technique described in section 3. We set $N = 2^4$ and perform a simulation with $m = 2^8$ time steps and final simulation time $T = 1/4$. The outcome, for two different choices of advection parameter ($b = -0.01$ and $b = -1$), is summarized in Figure 6, and the resulting values of λ actually employed in the experiments are given in Table 4.

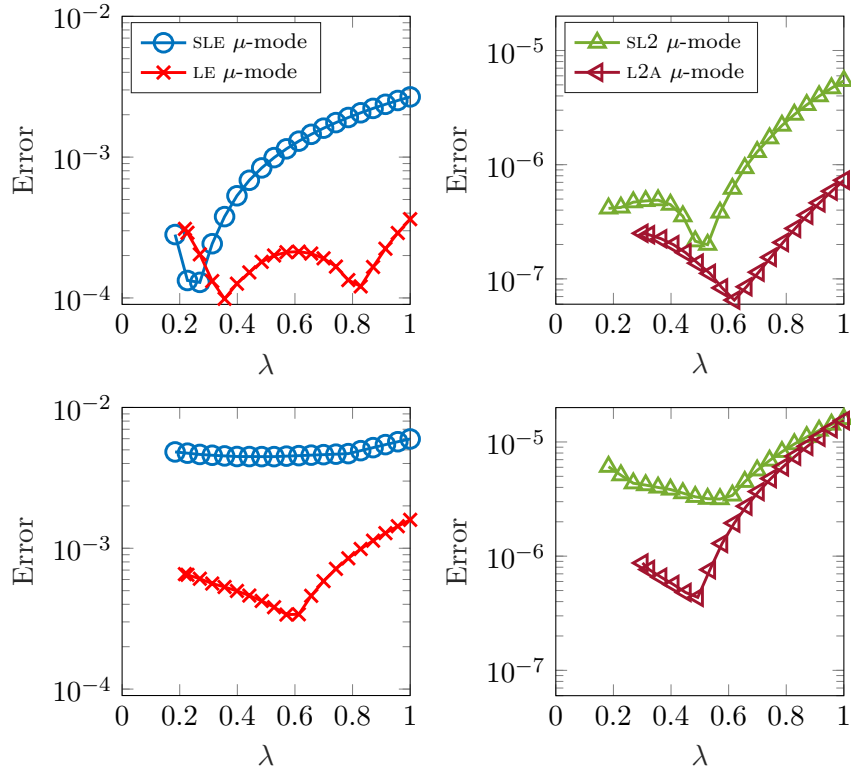


Figure 6: Solution of problem (19) rewritten as equation (20), with various first order schemes (left) and second order schemes (right), for different values of λ . The number of time steps is fixed to $m = 2^8$ for each method, while the number of degrees of freedom for each spatial variable is $N = 2^4$. The advection parameter is either $b = -0.01$ (top) or $b = -1$ (bottom).

	$b = -0.01$				$b = -1$			
	LE	SLE	L2A	SL2	LE	SLE	L2A	SL2
value of λ	0.36	0.27	0.62	0.53	0.60	0.50	0.50	0.57

Table 4: Values of λ for the different schemes that are employed to integrate problem (19) rewritten as equation (20) (see also Figure 6).

For the performance results, we set the number of uni-directional degrees of freedom to

$N = 60$. As term of comparison, we consider here the same time integrators but applied to the original equation (19) spatially discretized with second order centered finite differences. In addition, in this formulation, we also present the results obtained with the exponential Euler scheme, with the exponential RK2 with φ_1 integrator (with $c_2 = 1$) and with the two IMEX schemes. We perform the simulations with a number of time integration steps equal to 2^{ℓ_1} , with $\ell_1 = 9, \dots, 12$, for the first order methods, while we consider 2^{ℓ_2} , with $\ell_2 = 5, \dots, 8$, for the second order schemes. Again, the final simulation time is set to $T = 1/4$. The outcome of the experiments with advection parameter $b = -0.01$ is collected in a CPU diagram in Figure 7.

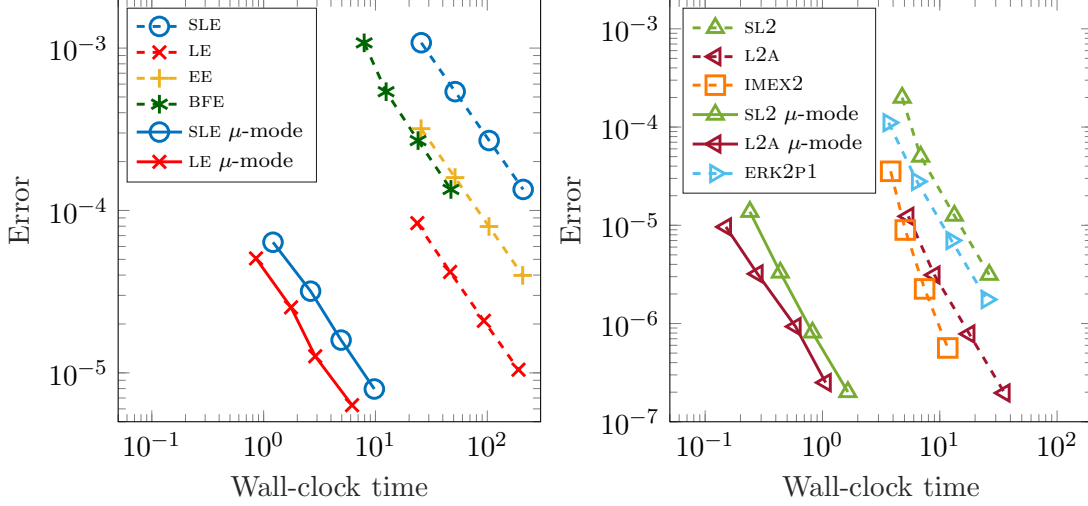


Figure 7: Results for the simulations of problem (19) (dashed lines), rewritten as equation (20) (solid lines), with $b = -0.01$ and different integrators of first order schemes (left, number of time steps $m = 2^{\ell_1}$ with $\ell_1 = 9, \dots, 12$) and second order schemes (right, number of time steps $m = 2^{\ell_2}$ with $\ell_2 = 5, \dots, 8$).

First of all, concerning the schemes of first order, we observe that in the original formulation (i.e., the dashed lines in the plot) the Lawson–Euler scheme is the one which performs best. Indeed, comparing it with the other exponential methods, it is the one which reaches the smallest error, with basically the same computational time. The backward-forward Euler method performs slightly better in terms of wall-clock time, but the reached accuracy is lower than for both the exponential Euler and the Lawson–Euler scheme. Hence, overall, it is not the preferred method. In any case, we observe that the proposed approach, i.e., solving instead equation (20) with μ -mode techniques (solid lines) is effective. Indeed, in this formulation both the Lawson–Euler and the stabilized Lawson–Euler methods perform better than the corresponding counterparts, both in terms of error and of wall-clock time, with a slight advantage for the former. Similar considerations can be drawn for the second order schemes. In fact, using the proposed approach, the Lawson2a scheme performs best, with a considerable advantage in performance in the μ -mode realization.

We then repeat the experiment by changing only the advection parameter, i.e., setting it to $b = -1$. The results are collected in Figure 8. In this advection dominated case, we first of all note that the stabilized schemes applied to equation (20) show errors which are either comparable (stabilized Lawson–Euler) or even lower (stabilized Lawson2) with respect to their counterparts in the original formulation. This is not true for the Lawson–Euler and the Lawson2a schemes, which in fact increase the errors when employing the proposed approach. Nevertheless, the gain in computational time is so considerable that overall the μ -mode implementation is the preferred one. In particular, the methods which perform best are the Lawson–Euler scheme

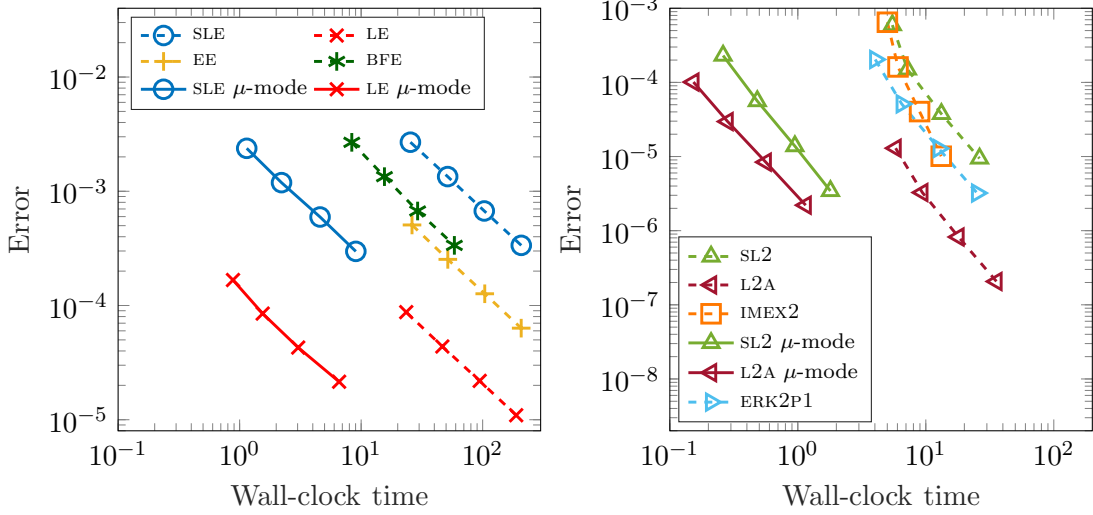


Figure 8: Results for the simulations of problem (19) (dashed lines), eventually rewritten as equation (20) (solid lines), with $b = -1$ and different integrators of first order (left, number of time steps $m = 2^{\ell_1}$ with $\ell_1 = 9, \dots, 12$) and second order (right, number of time steps $m = 2^{\ell_2}$ with $\ell_2 = 5, \dots, 8$).

and the Lawson2a method for first and second order, respectively.

6 Conclusion

In this manuscript, we presented an effective approach to solve advection-diffusion-reaction equations in the context of exponential integrators. It is based on a reformulation of the equation which allows for the employment of more efficient methods (FFT or μ -mode based techniques, for instance) to integrate it numerically. The conducted numerical examples in one, two, and three space dimension show the superiority of the approach. In addition, we presented two new schemes of Lawson type which have improved unconditional stability bounds compared to methods already available.

As a future challenge, we would like to study more in depth different choices for the approximation operator A (changing it according to the time evolution of the solution, for instance), both from a theoretical and a practical point of view. Also, we plan to apply the proposed approach to different classes of PDEs arising from science and engineering problems.

Acknowledgments

M. C. and F. C. acknowledge partial support from the Program Ricerca di Base 2019 No. RBVR199YFL of the University of Verona entitled “Geometric Evolution of Multi Agent Systems”; L. E. acknowledges support from the Austrian Science Fund (FWF) — project id: P32143-N32.

Appendix

For the convenience of the reader, we list here the integrators that have been mentioned and studied in the paper. We suppose that the equation under study is given in the following

abstract form

$$u'(t) = Au(t) + g(t, u(t)) = F(t, u(t)),$$

where A is a generic linear operator and g is a nonlinear function.

Lawson-type exponential integrators

The *Lawson–Euler* scheme is given by

$$u^{n+1} = e^{\tau A}(u^n + \tau g(t_n, u^n)).$$

The *stabilized Lawson–Euler* scheme is given by

$$u^{n+1} = u^n + \tau e^{\tau A} F(t_n, u^n).$$

The *Lawson2a* scheme is given by

$$U = e^{\frac{\tau}{2}A} \left(u^n + \frac{\tau}{2} g(t_n, u^n) \right), \quad u^{n+1} = e^{\tau A} u^n + \tau e^{\frac{\tau}{2}A} g \left(t_n + \frac{\tau}{2}, U \right).$$

The *Lawson2b* scheme is given by

$$U = e^{\tau A} (u^n + \tau g(t_n, u^n)), \quad u^{n+1} = e^{\tau A} u^n + \frac{\tau}{2} e^{\tau A} g(t_n, u^n) + \frac{\tau}{2} g(t_n + \tau, U).$$

The *stabilized Lawson2* scheme is given by

$$U = u^n + \alpha \tau e^{\alpha \tau A} F(t_n, u^n), \quad u^{n+1} = u^n + \tau e^{\frac{\tau}{2}A} F(t_n, u^n) + \frac{\tau}{2\alpha} e^{\tau A} (g(t_n + \alpha \tau, U) - g(t_n, u^n)).$$

Classical exponential integrators

The *exponential Euler* scheme is given by

$$u^{n+1} = u^n + \tau \varphi_1(\tau A) F(t_n, u^n).$$

The *exponential Runge–Kutta* scheme of second order involving the φ_2 function is given by

$$\begin{aligned} U &= u^n + c_2 \tau \varphi_1(c_2 \tau A) F(t_n, u^n), \\ u^{n+1} &= u^n + \tau \varphi_1(\tau A) F(t_n, u^n) + \frac{\tau}{c_2} \varphi_2(\tau A) (g(t_n + c_2 \tau, U) - g(t_n, u^n)). \end{aligned}$$

The *exponential Runge–Kutta* scheme of second order involving the φ_1 function is given by

$$\begin{aligned} U &= u^n + c_2 \tau \varphi_1(c_2 \tau A) F(t_n, u^n), \\ u^{n+1} &= u^n + \tau \varphi_1(\tau A) F(t_n, u^n) + \frac{\tau}{2c_2} \varphi_1(\tau A) (g(t_n + c_2 \tau, U) - g(t_n, u^n)). \end{aligned}$$

IMEX schemes

The *backward-forward Euler* scheme is given by

$$(I - \tau A) u^{n+1} = u^n + \tau g(t_n, u^n).$$

The second order *implicit-explicit2* scheme proposed in reference [29] is given by

$$\left(I - \frac{\tau}{2} A \right) U = u^n + \frac{\tau}{2} g(t_n, u^n), \quad \left(I - \frac{\tau}{2} A \right) u^{n+1} = u^n + \frac{\tau}{2} A u^n + \tau g \left(t_n + \frac{\tau}{2}, U \right).$$

References

- [1] A. H. Al-Mohy and N. J. Higham. Computing the action of the matrix exponential, with an application to exponential integrators. *SIAM J. Sci. Comput.*, 33(2):488–511, 2011.
- [2] S. Badia, A. F. Martín, and R. Planas. Block recursive LU preconditioners for the thermally coupled incompressible inductionless MHD problem. *J. Comput. Phys.*, 274:562–591, 2014.
- [3] M. Caliari, F. Cassini, L. Einkemmer, A. Ostermann, and F. Zivcovich. A μ -mode integrator for solving evolution equations in Kronecker form. *J. Comput. Phys.*, 455:110989, 2022.
- [4] M. Caliari, F. Cassini, and F. Zivcovich. Approximation of the matrix exponential for matrices with a skinny field of values. *BIT Numer. Math.*, 60(4):1113–1131, 2020.
- [5] M. Caliari, F. Cassini, and F. Zivcovich. BAMPHI: Matrix and transpose free action of the combinations of φ -functions from exponential integrators. *J. Comput. Appl. Math.*, 423:114973, 2023.
- [6] M. Caliari, F. Cassini, and F. Zivcovich. A μ -mode BLAS approach for multidimensional tensor structured problems. *Numer. Algorithms*, 92(4):2483–2508, 2023.
- [7] M. Caliari, P. Kandolf, A. Ostermann, and S. Rainer. The Leja method revisited: backward error analysis for the matrix exponential. *SIAM J. Sci. Comput.*, 38(3):A1639–A1661, 2016.
- [8] M. Caliari, M. Vianello, and L. Bergamaschi. Interpolating discrete advection–diffusion propagators at Leja sequences. *J. Comput. Appl. Math.*, 172(1):79–99, 2004.
- [9] P. Castillo and Y. Saad. Preconditioning the matrix exponential operator with applications. *J. Sci. Comput.*, 13(3):275–302, 1998.
- [10] L. Chacón, D. A. Knoll, and J. M. Finn. An implicit, nonlinear reduced resistive MHD solver. *J. Comput. Phys.*, 178(1):15–36, 2002.
- [11] M. Chen and D. Kressner. Recursive blocked algorithms for linear systems with Kronecker product structure. *Numer. Algorithms*, 84:1199–1216, 2020.
- [12] C. Clancy and J. A. Pudykiewicz. On the use of exponential time integration methods in atmospheric models. *Tellus A: Dyn. Meteorol. and Oceanogr.*, 65(1):20898, 2013.
- [13] E. C. Cyr, J. N. Shadid, and R. S. Tuminaro. Teko: A block preconditioning capability with concrete example applications in Navier–Stokes and MHD. *SIAM J. Sci. Comput.*, 38(5):S307–S331, 2016.
- [14] P. J. Deka and L. Einkemmer. Exponential integrators for resistive magnetohydrodynamics: Matrix-free Leja interpolation and efficient adaptive time stepping. *Astrophys. J. Suppl. Ser.*, 259(2):57, 2022.
- [15] L. Einkemmer, M. Tokman, and J. Loffeld. On the performance of exponential integrators for problems in magnetohydrodynamics. *J. Comput. Phys.*, 330:550–565, 2017.
- [16] M. Frigo and S. G. Johnson. FFTW: an adaptive software architecture for the FFT. In *Proceedings of the 1998 IEEE International Conference on Acoustics, Speech and Signal Processing (ICASSP '98)*, pages 1381–1384. IEEE, 1998.

- [17] S. Gaudreault, G. Rainwater, and M. Tokman. KIOPS: A fast adaptive Krylov subspace solver for exponential integrators. *J. Comput. Phys.*, 372:236–255, 2018.
- [18] V. Grimm and M. Hochbruck. Rational approximation to trigonometric operators. *BIT Numer. Math.*, 48(2):215–230, 2008.
- [19] M. Hochbruck and C. Lubich. On Krylov subspace approximations to the matrix exponential operator. *SIAM J. Numer. Anal.*, 34(5):1911–1925, 1997.
- [20] M. Hochbruck and A. Ostermann. Exponential integrators. *Acta Numer.*, 19:209–286, 2010.
- [21] J. D. Lawson. Generalized Runge-Kutta processes for stable systems with large Lipschitz constants. *SIAM J. Numer. Anal.*, 4(3):372–380, 1967.
- [22] J. Loffeld and M. Tokman. Comparative performance of exponential, implicit, and explicit integrators for stiff systems of ODEs. *J. Comput. Appl. Math.*, 241:45–67, 2013.
- [23] V. T. Luan, J. A. Pudykiewicz, and D. R. Reynolds. Further development of efficient and accurate time integration schemes for meteorological models. *J. Comput. Phys.*, 376:817–837, 2019.
- [24] J. Niesen and W. M. Wright. Algorithm 919: A Krylov subspace algorithm for evaluating the ϕ -functions appearing in exponential integrators. *ACM Trans. Math. Softw.*, 38(3):1–19, 2012.
- [25] G. Papanicolau and X. Xin. Reaction–diffusion fronts in periodically layered media. *J. Stat. Phys.*, 63:915–931, 1991.
- [26] D. R. Reynolds, R. Samtaney, and C. S. Woodward. Operator-based preconditioning of stiff hyperbolic systems. *SIAM J. Sci. Comput.*, 32(1):150–170, 2010.
- [27] Y. Saad. *Iterative Methods for Sparse Linear Systems*. SIAM, Philadelphia, 2nd edition, 2003.
- [28] J. Van Den Eshof and M. Hochbruck. Preconditioning Lanczos approximations to the matrix exponential. *SIAM J. Sci. Comput.*, 27(4):1438–1457, 2006.
- [29] H. Wang, Q. Zhang, S. Wang, and C.-W. Shu. Local discontinuous Galerkin methods with explicit-implicit-null time discretizations for solving nonlinear diffusion problems. *Sci. China Math.*, 63:183–204, 2020.
- [30] J. Xu and L. Zikatanov. Algebraic multigrid methods. *Acta Numer.*, 26:591–721, 2017.